International Journal of Earth, Energy and Environmental Sciences
ISSN: 2517-942X
Vol:11, No:1, 2017

Two-Dimensional Observation of Oil Displacement by Water in a Petroleum Reservoir through Numerical Simulation and Application to a Petroleum Reservoir

Ahmad Fahim Nasiry, Shigeo Honma

***Abstract*—**We examine two-dimensional oil displacement by water in a petroleum reservoir. The pore fluid is immiscible, and the porous media is homogenous and isotropic in the horizontal direction. Buckley-Leverett theory and a combination of Laplacian and Darcy's law are used to study the fluid flow through porous media, and the Laplacian that defines the dispersion and diffusion of fluid in the sand using heavy oil is discussed. The reservoir is homogenous in the horizontal direction, as expressed by the partial differential equation. Two main factors which are observed are the water saturation and pressure distribution in the reservoir, and they are evaluated for predicting oil recovery in two dimensions by a physical and mathematical simulation model. We review the numerical simulation that solves difficult partial differential reservoir equations. Based on the numerical simulations, the saturation and pressure equations are calculated by the iterative alternating direction implicit method and the iterative alternating direction explicit method, respectively, according to the finite difference assumption. However, to understand the displacement of oil by water and the amount of water dispersion in the reservoir better, an interpolated contour line of the water distribution of the five-spot pattern, that provides an approximate solution which agrees well with the experimental results, is also presented. Finally, a computer program is developed to calculate the equation for pressure and water saturation and to draw the pressure contour line and water distribution contour line for the reservoir.

***Keywords*—**Numerical simulation, immiscible, finite difference, IADI, IADE, waterflooding.

I. Introduction

TO develop prediction systems for oil recovery, the widely used method is modified by Buckley-Leverett theory and it is known as the waterflooding technique where water is injected into the petroleum reservoir to increase oil production [1]. Fig. 1 shows the waterflooding system for injection and production wells in two dimensions horizontally. For clear observations, the arrangement of the wells should be considered because it improves pumping and makes calculations easier [2].

As water approaches the oil reservoir, the conditions become complex because the liquids are immiscible, and only numerical methods can calculate the liquid behavior by approximation theory [4]. The two main factors are pressure and saturation. The relative permeability is also a key factor in controlling the fluid distribution location in the reservoir and is a function of water saturation that can be obtained by laboratory measurements. The most suitable equation for treating reservoir conditions in two dimensions is the Laplace equation under Darcy's law combined with Buckley-Leverett theory [5]. Because the partial differential equation of an immiscible reservoir is developed, a numerical method is the best way to obtain a solution. After that, the reservoir is modeled as a block that is divided into meshes because the finite difference approximates the equations at every node of the meshes. After this system has been developed, calculation of the saturation and pressure equations becomes easy.

N. Ahmad Fahim is a graduate student of Tokai University Environmental and Civil Engineering Department, (phone: 07021776969, e-mail: fahimnasiry@yahoo.com).

S. Honma is a Professor at Civil Engineering Department Tokai University, Japan (phone: 09025581965, e-mail: shigeohonma@hotmail.com).

II. Simple Geometry of Reservoir Conditions for the Simulation Model

The reservoir conditions are described by simple geometry. The reservoir is 60 cm long and 40 cm wide, and is bounded by two impervious boundaries and two constant heads. Fig. 2 shows a schematic of the geometry including the injection well and production wells. The distance between wells is 20 cm in the length direction and 10 cm in the width direction. The geometry is used to create a simulation model (Fig. 3) for a laboratory experiment to investigate the reservoir behavior and measure the physical characteristics of the water displacement in two dimensions.

III. Experimental Apparatus for Demonstrating Fluid Flow Characteristic in Theora Sand

A regular, flat rectangular simulation model is used according to Darcy's law to calculate fluid flow through a uniform aquifer of Theora sand that is 60 cm long, 40 cm wide, and 3 cm thick (Fig. 3). The positions of the injection well and production wells in the model and the distance between the wells are specified. To control the pumping, the wells are connected to a piezometer that measures the hydraulic differences between wells. This model is designed for studying groundwater flow characteristics by measuring the flow of water through the sand to investigate groundwater pollution and groundwater management. Under the geological assumption, two areas with petroleum reservoirs and the same groundwater conditions should have the same settling of the reservoirs. Hence, this simulation model can be used also for investigating petroleum reservoir behavior. First, the model was filled with a known amount of Theora sand (unit: grams), and then completely saturated with oil. The hydraulic head was fixed

according to the piezometer, which was connected to the individual wells (Fig. 3). The pumping rate for the injection well was changed in steps of 0.275 cm^3/s, production wells were opened with the initial reservoir condition, and the rate for the wells were changed in steps of 0.14–0.19 cm^3/s. The distance between the injection and production wells was constant (22.36 cm), owing to the homogeneity of the reservoir so that the breakthrough time could be predicted in every well.

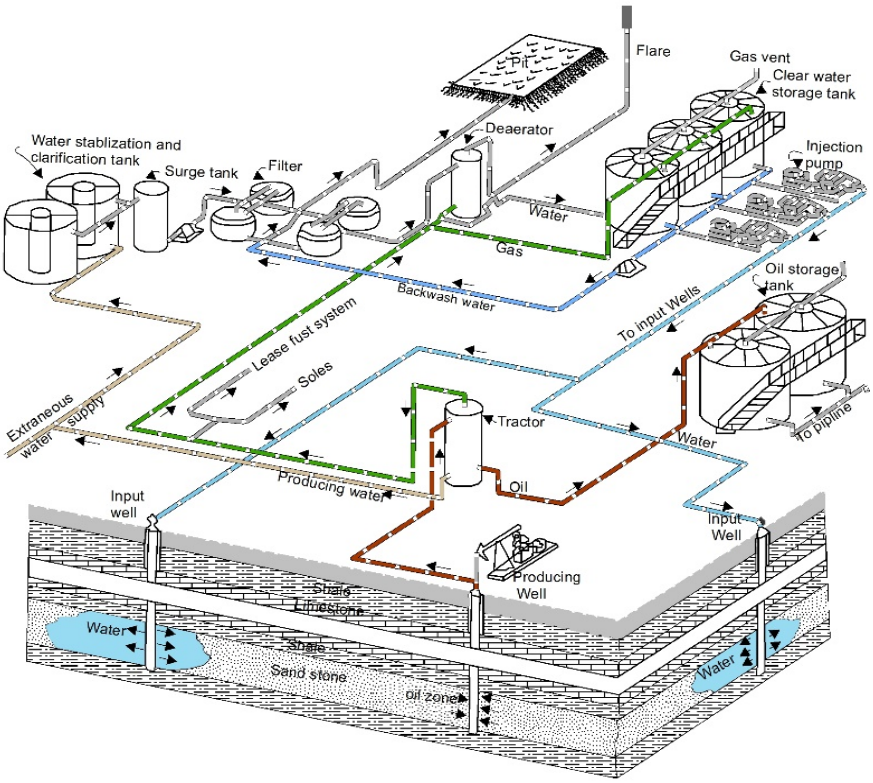

Fig. 1 Schematic diagram of the main equipment for a closed-system water injection project [3]

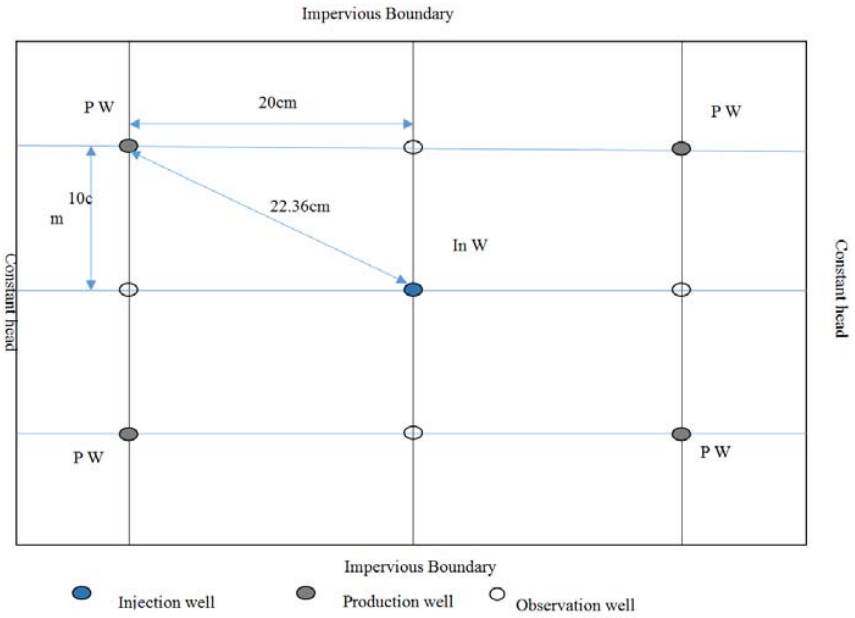

Fig. 2 Simple geometry of the reservoir conditions

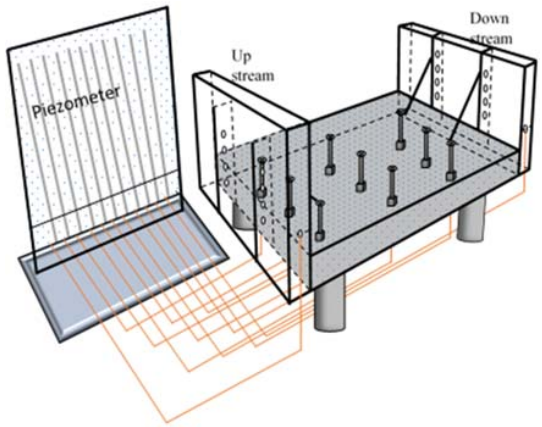

Fig. 3 Experimental apparatus

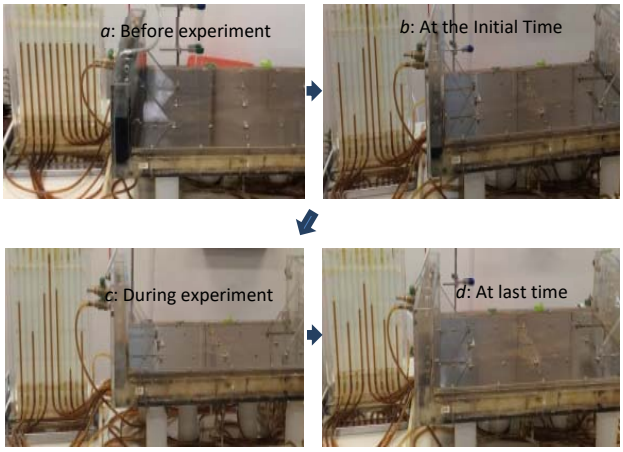

Fig. 4 Five spot pattern: one injection well and four production wells

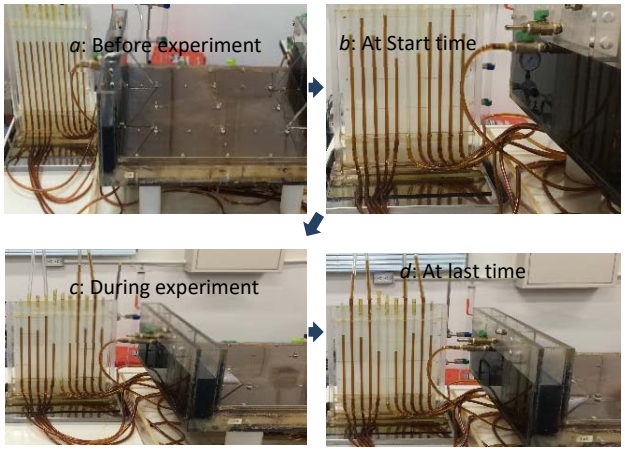

Fig. 5 Five-spot pattern: four injection wells and one production well

To simplify the calculation, the pumping ratio was kept equal to the total sum of the production wells. At the end, the total volume of oil produced by water injected into the reservoir was about 1195 cm^3, which was broadly consistent with Buckley-Leverett theory. Figs. 4 (a)-(d) and 5 (a)-(d) show photographs of the experiment and demonstrate the water displacement of the five-spot pattern. The piezometer data for the wells observed during operation defined the relationship between immiscible water and oil in homogenous porous materials. Finally, according to the piezometer head data recorded during pumping, the equipotential lines were interpolated by an approximation method. The streamline used to determine the saturation front was plotted by connecting the pressure drop points during production (Figs. 11 (a)-(c) and 12 (a), (b)).

IV. Equation Development for an Incompressible Flow of Oil and Water

According to Darcy's law, the flow equations of fluid oil and water were developed via Buckley-Leverett frontal displacement theory. The saturation equation for oil and water through porous media with respect to the mobility factor between two phases in two dimensions is

$$\frac{\partial}{\partial x}\left(k_x\lambda_w\frac{\partial pw}{\partial x}\right)+\frac{\partial}{\partial y}\left(k_x\lambda_w\frac{\partial pw}{\partial y}\right)=\phi\frac{\partial S_w}{\partial t} \quad (1)$$

$$\frac{\partial}{\partial x}\left(k_x\lambda_o\frac{\partial po}{\partial x}\right)+\frac{\partial}{\partial y}\left(k_x\lambda_o\frac{\partial po}{\partial y}\right)=\phi\frac{\partial S_o}{\partial t} \quad (2)$$

where k_x and k_y are the intrinsic permeabilities of the medium in the x and y directions, respectively, $\lambda_w=\frac{k_{rw}}{\mu w}$ and $\lambda_o=\frac{k_{ro}}{\mu o}$ are the mobility factors for oil and water, respectively, and P_o and p_w are the fluid pressures for oil and water, respectively.

The commune relationship between saturation and pressure is $S_w+S_o=1$, and $p_o-p_w=p_o/p_w$. When capillary pressure po/w is neglected because it is small, namely $p_o=p_w=p$, water and oil pressure is p, and (1) and (2) take the forms

$$\frac{\partial}{\partial x}\left(k_x\lambda_w\frac{\partial p}{\partial x}\right)+\frac{\partial}{\partial y}\left(k_x\lambda_w\frac{\partial p}{\partial x}\right)=\phi\frac{\partial S_w}{\partial t} \quad (3)$$

$$\frac{\partial}{\partial x}\left(k_x\lambda_o\frac{\partial p}{\partial x}\right)+\frac{\partial}{\partial y}\left(k_x\lambda_o\frac{\partial p}{\partial x}\right)=\phi\frac{\partial S_o}{\partial t} \quad (4)$$

If the oil and water saturation relationship, $S_w+S_o=1$, is substituted into the right-hand side of (4) and the saturation term is canceled, the sum of the oil and water equations of (3) and (4) is

$$\frac{\partial}{\partial x}\left\{k_x(\lambda_w+\lambda_o)\frac{\partial p}{\partial x}\right\}+\frac{\partial}{\partial y}\left\{k_y(\lambda_w+\lambda_o)\frac{\partial p}{\partial y}\right\}=0 \quad (5)$$

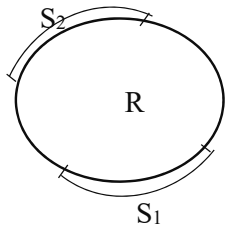

Fig. 6 Schematic of the boundary condition

Equation (5) is a steady state equation unsuitable for unsteady states that show pressure changes over time, and where the water saturation is controlled by mobility factors.

The treatment of k_{ro} and k_{rw} oil and water relative permeability that are evaluated at $k+\frac{1}{2}$ in a complete form applying $S_w^{k+\frac{1}{2}}$ k_{rw}, k_{ro} are evaluated at $k+\frac{1}{2}$ using $S_w^{k+\frac{1}{2}}$

$$\text{IC: } p = p_o \text{ in R} \tag{6}$$

$$\text{BC: } p = \hat{p} \text{ on } S_1 \text{ Fig. 6.} \tag{7a}$$

For evaluating the boundary condition at S_2

$$k_x(\lambda_w+\lambda_o)\frac{\partial p}{\partial x}nx + k_x(\lambda_w+\lambda_o)\frac{\partial p}{\partial x}ny = \frac{\ddot{Q}T}{A} \tag{7b}$$

Equation (5) is solved and converted to a finite number. Let $\lambda_{o/w}=\lambda_w+\lambda_o$ upstream.

V. Numerical Simulation

Analytical solutions are limited to simple idealized conditions so that the flow equation can be solved. For example, a single well that is homogenous and isotropic in the horizontal direction. Numerical simulation is increasingly used in the petroleum industry, and its accuracy has been proved by comparison with complex partial differential equations for petroleum reservoirs [6]. This has demonstrated that Buckley–Leverett theory for simultaneous two-phase flow is improved by using numerical simulations that can solve complex partial differential equations for petroleum reservoir. Finite difference methods, namely the iterative alternating direction implicit (IADI) method and the iterative alternating direction explicit (IADE) method, are used to account for the saturation and pressure equations, respectively, and to approximate the areal distribution of water displacement for oil recovery from the reservoir in the region.

VI. Finite Difference Method

Numerical methods are used to solve the discretized partial differential equations considering time and space. The finite differences methods approximate the solution of partial differential equations of fluid flow of liquid simultaneously through porous media in a rectangle divided into a grid, and these methods have long been used for decisions about production reservoir contents. The finite difference method replaces the partial differential equation of flow with a set of finite difference equations in discretized time and space (Fig. 7) [7].

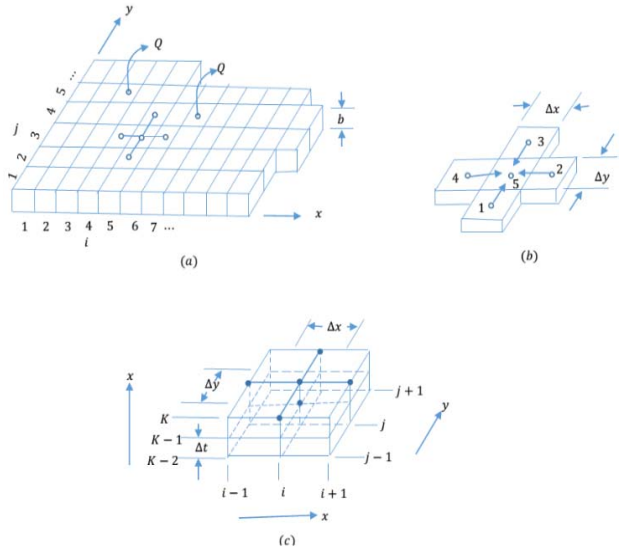

Fig. 7 Scheme of finite differences in two dimensions

Equation (5) is the two-phase flow, which describes the mobility ratio and pressure gradient in two dimensions in an isotropic-homogeneous incompressible medium with respect to the mobility ratio and pressure gradient.

A general schematic of the finite difference method is shown in Fig. 7. The partial differential equation of the transient flow of oil and water under Laplacian equation (7b) now can be transformed into a finite difference equation that considers the mobility ratio that controls the fluid distribution and the pressure gradients that includes *p*.

$$\frac{1}{\Delta x}\left\{k_x\left(A\lambda_{o/wi+1,j}+A\lambda_{o/wij}\right)\frac{p_{i+1,j}^{k+1/2}-p_{i,j}^{k+1/2}}{\Delta x}-k_x\left(A\lambda_{o/wij}+A\lambda_{o/wi-1,j}\right)\frac{p_{i+1,j}^{k+1/2}-p_{i-1,j}^{k+1/2}}{\Delta x}\right\}+$$
$$\frac{1}{\Delta y}\left\{k_y\left(B\lambda_{o/wij+1}+B\lambda_{o/wij}\right)\frac{p_{i,j+1}^{k+1/2}-p_{i,j}^{k+1/2}}{\Delta y}-k_y\left(B\lambda_{o/wij}+B\lambda_{o/wij-1}\right)\frac{p_{i,j}^{k+1/2}-p_{i,j-1}^{k+1/2}}{\Delta y}\right\}=0 \tag{8}$$

Let $\Delta x=\Delta y$, $k_x=k_y$, so $k=\frac{k_x}{\Delta x^2}=\frac{k_y}{\Delta y^2}$. Here, substituting the time derivative for k in both sides of (8) gives

$$k\left(A\lambda_{o/wi+1,j}+A\lambda_{o/wij}\right)p_{i+1,j}^{k+1/2}-p_{i,j}^{k+1/2}-\left(A\lambda_{o/wij}+A\lambda_{o/wi-1,j}\right)p_{i+1,j}^{k+1/2}-p_{i-1,j}^{k+1/2}+$$
$$k\left(B\lambda_{o/wij+1}+B\lambda_{o/wij}\right)p_{i,j+1}^{k+1/2}-p_{i,j}^{k+1/2}-\left(B\lambda_{o/wij}+B\lambda_{o/wij-1}\right)p_{i,j}^{k+1/2}-p_{i,j-1}^{k+1/2}=0 \tag{9}$$

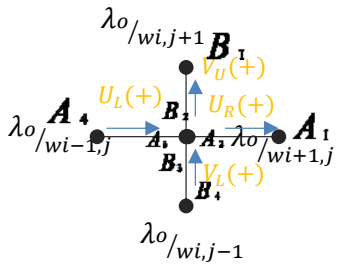

Fig. 8 Scheme for stream direction

The coefficients A_1 to A_4 and B_1 to B_4 are introduced to clarify the region of flow in finite differences, Fig. 8 illustrates the locations of the coefficients.

$$\begin{aligned} U_R>0, A_1=0, A_2=1 \\ U_R<0, A_1=1, A_2=0 \\ V_U>0, A_3=0, A_4=1 \\ V_U<0, A_3=1, A_4=0 \\ U_L>0, B_1=0, B_2=1 \\ U_L<0, B_1=1, B_2=0 \\ V_L>0, B_3=0, B_4=1 \\ V_L<0, B_3=1, B_4=0 \end{aligned} \tag{10}$$

Thus, the mobility factors for A_U upstream and A_D downstream in the x direction and B_U upstream and B_D downstream in the y direction are shown by specific coefficients. Let,

$$\begin{aligned} A_1\lambda_{o/wi+1,j}+A_2\lambda_{o/wi,j}=A_U \\ B_1\lambda_{o/wi,j+1}+B_2\lambda_{o/wi,j}=B_U \\ B_3\lambda_{o/wi,j}+B_4\lambda_{o/wi,j-1}=B_D \\ A_3\lambda_{o/wi,j}+A_4\lambda_{o/wi-1,j}=A_D \\ A_U\left(p_{i+1,j}^{k+1/2}-p_{i,j}^{k+1/2}\right)-A_D\left(p_{i,j}^{k+1/2}-p_{i-1,j}^{k+1/2}\right)+ \\ B_U\left(p_{i,j+1}^{k+1/2}-p_{i,j}^{k+1/2}\right)-B_D\left(p_{i,j}^{k+1/2}-p_{i,j-1}^{k+1/2}\right)=0 \end{aligned} \tag{11}$$

The time step level for computing p was selected at $k+1/2$ because the pressure change in flow (15) and (16) should be evaluated between k and $k+1$.

$$A_U p_{i+1,j}+A_D p_{i-1,j}+B_U p_{i,j+1}+B_D p_{i,j-1}=4\left(A_U+A_D+B_U+B_D\right)p_{i,j} \tag{12}$$

Process for Success Over-Relaxation (SOR)

1) Specify $p_{i,j}^{k+1/2}$ for the region according to the initial and boundary conditions.
2) Compute residual $\varepsilon_{i,j}$

$$\varepsilon_{i,j}=4\left(A_U+A_D+B_U+B_D\right)p_{i,j}^{k+1/2}-A_U p_{i+1,j}^{k+1/2}-A_D p_{i-1,j}^{k+1/2}-B_U p_{i,j+1}^{k+1/2}-B_D p_{i,j-1}^{k+1/2}$$

3) Modify $p_{i,j}^{k+1/2}$ so that

$$p_{i,j}^{k+1/2}=p_{i,j}^{k+1/2}-f\frac{\varepsilon_{i,j}}{4} \quad f=0.1\sim1.2.$$

Over-relaxation factor. Repeat steps 2 and 3 until the $\varepsilon_{i,j}$ values settle to within a prescribed tolerance (until $p_{i,j}^{k+1/2}$ converge). Solve water saturation (3). Recall that

$$\begin{aligned} \lambda_w=\frac{k_{rw}}{\mu w} \\ k_x=k_y \\ \frac{k_x}{\Delta x}\left\{\left(A_1\lambda_{wi+1,j}+A_2\lambda_{wij}\right)\frac{p_{i+1,j}^{k+1/2}-p_{i,j}^{k+1/2}}{\Delta x}-\left(A_3\lambda_{wij}+A_4\lambda_{wi-1,j}\right)\frac{p_{i+1,j}^{k+1/2}-p_{i-1,j}^{k+1/2}}{\Delta x}\right\}+ \\ \frac{k_y}{\Delta y}\left\{\left(B_1\lambda_{wij+1}+B_2\lambda_{wij}\right)\frac{p_{i,j+1}^{k+1/2}-p_{i,j}^{k+1/2}}{\Delta y}-\left(B_3\lambda_{wij}+B_4\lambda_{wij-1}\right)\frac{p_{i,j}^{k+1/2}-p_{i,j-1}^{k+1/2}}{\Delta y}\right\}=\Phi\frac{S_{wij}^{k+1}-S_{wij}^{k}}{\Delta t} \end{aligned} \tag{13}$$

Coefficients $A_1\sim B_4$ are the same as in (10). Let $\gamma=\frac{k_x\Delta t}{\Delta x^2}=\frac{k_x\Delta t}{\Delta y^2}$

$$\begin{aligned} A_1\lambda_{wi+1,j}+A_2\lambda_{wi,j}=C_U \\ B_1\lambda_{wi,j+1}+B_2\lambda_{wi,j}=D_U \\ B_3\lambda_{wi,j}+B_3\lambda_{wi,j-1}=D_D \\ A_3\lambda_{wi,j}+A_4\lambda_{wi-1,j}=C_D \\ \frac{\gamma}{\phi}\left\{\begin{matrix} C_U\left(p_{i+1,j}-p_{i,j}\right)-C_D\left(p_{i,j}-p_{i-1,j}\right)- \\ D_U\left(p_{i,j+1}-p_{i,j}\right)-D_D\left(p_{i,j}-p_{i,j-1}\right) \end{matrix}\right\}=S_{wi,j}^{k+1}-S_{wi,j}^{k} \\ S_{wi,j}^{k+1}=S_{wi,j}^{k}+\frac{\gamma}{\phi}\left\{\begin{matrix} C_U p_{i+1,j}^{k+1/2}+C_D p_{i-1,j}^{k+1/2}+D_U p_{i,j+1}^{k+1/2}+ \\ D_D p_{i,j-1}^{k+1/2}-\left(C_U+C_D+D_U+D_D\right)p_{i,j}^{k+1/2} \end{matrix}\right\} \end{aligned} \tag{14}$$

VII. IADI Method

One popular method of solving nodal equations iteratively is the IADI method [8], which is used for calculation iterations of rows and columns in the matrix based on the equation. The calculation procedure is shown below.

Equation (5) is solved as follows by the IADI method. Let $\lambda_{o/w}=\lambda_w+\lambda_o$ upstream. For the *x*-direction (*i*-direction)

$$\begin{aligned} \frac{1}{\Delta x}\left\{k_x\left(A_1\lambda_{wi+1,j}^{k+1/2}+A_2\lambda_{wij}^{k+1/2}\right)\frac{p_{i+1,j}^{k+1/2}-p_{ij}^{k+1/2}}{\Delta x}-k_x\left(A_3\lambda_{wij}^{k+1/2}+A_4\lambda_{wi-1,j}^{k+1/2}\right)\frac{p_{ij}^{k+1/2}-p_{i-1,j}^{k+1/2}}{\Delta x}\right\}+ \\ \frac{1}{\Delta y}\left\{k_y\left(B_1\lambda_{wij+1}^{k+1/2}+B_2\lambda_{wij}^{k+1/2}\right)\frac{p_{i,j+1}^{k+1/2}-p_{ij}^{k+1/2}}{\Delta y}-k_y\left(B_3\lambda_{wij}^{k+1/2}+B_4\lambda_{wij-1}^{k+1/2}\right)\frac{p_{ij}^{k+1/2}-p_{i,j-1}^{k+1/2}}{\Delta y}\right\}=0 \end{aligned} \tag{15}$$

The coefficients $A_1\sim A_4$ are evaluated at $k+1/2$ and $B_1\sim B_4$ are evaluated at k.

$$U_R^{k,k+1/2} > 0 \rightarrow A_1 = 0, A_2 = 1,$$
$$\text{Namely } p_{i,j} > p_{j+1,j}.$$
$$U_R > 0, A_1 = 0, A_2 = 1,\ U_R < 0, A_1 = 1, A_2 = 0$$
$$V_U > 0, A_3 = 0, A_4 = 1,\ V_U < 0, A_3 = 1, A_4 = 0$$
$$U_L > 0, B_1 = 0, B_2 = 1,\ U_L < 0, B_1 = 1, B_2 = 0 \quad (16)$$
$$V_L > 0, B_3 = 0, B_4 = 1,\ V_L < 0, B_3 = 1, B_4 = 0$$
$$\text{Let } \Delta x = \Delta y,\ k_x = k_y, \text{ so } k = \frac{k_x}{\Delta x^2} = \frac{k_y}{\Delta y^2}$$
$$k\left\{\begin{matrix}\left(A_1\lambda_{o/wi+1,j} + A_2\lambda_{o/wi,j}\right)^{k+1/2} p_{i+1,j}^{k+1/2} - p_{i,j}^{k+1/2} \\ -\left(A_3\lambda_{o/wi,j} + A_4\lambda_{o/wi-1,j}\right)^{k+1/2} p_{i,j}^{k+1/2} - p_{i-1,j}^{k+1/2}\end{matrix}\right\} +$$
$$k\left\{\begin{matrix}\left(B_1\lambda_{o/wi,j+1} + B_2\lambda_{o/wi,j}\right)^{k} p_{i,j+1}^{k} - p_{i,j}^{k} \\ -\left(B_3\lambda_{o/wi,j} + B_4\lambda_{o/wi,j-1}\right)^{k} p_{i,j}^{k} - p_{i,j-1}^{k}\end{matrix}\right\} = 0$$

Let

$$\left(A_1\lambda_{o/wi+1,j} + A_2\lambda_{o/wi,j}\right)^{k+1/2} = A_U^{k+1/2}$$
$$\left(A_3\lambda_{o/wi,j} + A_4\lambda_{o/wi-1,j}\right)^{k+1/2} = A_D^{k+1/2} \quad (17)$$
$$\left(B_1\lambda_{o/wi,j+1} + B_2\lambda_{o/wi,j}\right)^{k} = B_U^{k}$$
$$\left(B_3\lambda_{o/wi,j} + B_4\lambda_{o/wi,j-1}\right)^{k} = B_D^{k}$$

VIII. Pressure Distribution in the Reservoir in Two-Dimension

We examine oil displacement by water in two dimensions horizontally in a homogenous, isotropic medium with no mass transfer under the Laplace equation. The system has a five-spot pattern that includes an injection well and production wells, where the injection rate is equal to the total of the production rates in the steady sate. The pressure calculation according to (12) starts at time $t = 0$, and then it increases gradually until it converges. The calculation is based on a computer program. The space differences Δx and Δy are assumed to be equal intervals in the x and y-directions (Fig. 9). In homogenous porous media, the pressure is equal around the injection well at equal time intervals (Table I), which creates buffer contour lines (Fig. 10). As breakthrough approaches, the fluid flow pressure is dropped down. The water saturation and the water distribution contour line is directly affected by fluid flow pressure.

IX. Water Saturation Contour Line

As the water saturation equation is improved by the partial differential equation (14), it is considered to solve numerically the nonlinearity of the water saturation equation in two dimensions in a homogenous, isotropic medium horizontally. If the equation is solved by numerical simulation, the finite difference method is used to approximate the diffusion and dispersion of water and oil displacement in the reservoir with the Laplacian equation. However, developing a computer program for the finite difference equation of water saturation is difficult because the dispersion of water changes slightly in every portion of soil. A five-spot pattern arrangement of injection and production wells is used to observe the oil displacement by water in a petroleum reservoir. More details of the five-spot pattern are discussed elsewhere [9].

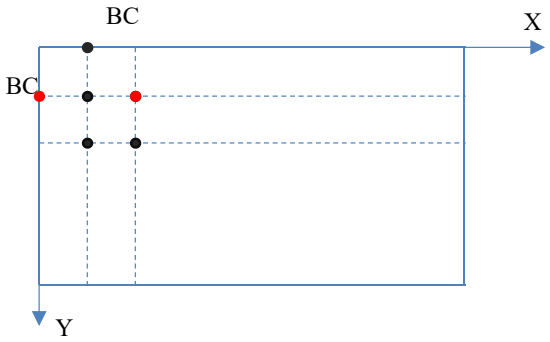

Fig. 9 Scheme of general grid construction for IADI

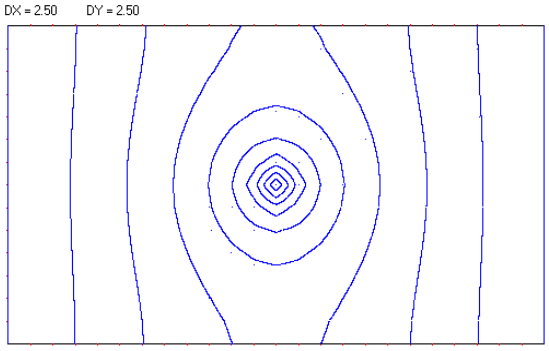

Fig. 10 Schematic of pressure contour lines drawn by a computer program

The injection well in the center has a rate 0.27 cm^3/s and the production wells in each quadrant have a rate of 0.14–0.19 cm^3/s.

The pumping operation started at time $t = 0$ and continued to 86 min, and the total volume of oil collected was about 1193.28 cm^3 from the total amount of oil of 3154.7 cm^3.

Based on the piezometer data for the wells (Figs. 11 (a)-(c), Table II) the equipotential line is drawn by the interpolation approximation method (Fig. 11 (a)). Streamlines are assumed to be perpendicular to the equipotential line [10], and a cross section (A-Á) is plotted (Fig. 11 (b)) showing the hydraulic head from the piezometer. The streamlines for the water distribution (blue, curved lines) are plotted according to the pressure drop interpolated across the production wells. Our results show that in two dimensions, approximately 39% of the total oil is recovered. To increase the amount of oil recovered from the reservoir, the pattern of the wells should be altered.

TABLE I
CALCULATION RESULTS FROM PRESSURE EQUATION

0,2	**0,2**	**0,2**	**0,2**	**0,2**	**0,2**	**0,2**	**0,2**	**0,3**	**0,3**	**0,3**	**0,2**	**0,2**	**0,2**	**0,2**	**0,2**	**0,2**	**0,2**	**0,2**
0,2	0,2	0,2	0,2	0,2	0,2	0,2	0,2	0,3	0,3	0,3	0,2	0,2	0,2	0,2	0,2	0,2	0,2	0,2
0,2	0,2	0,2	0,2	0,2	0,2	0,2	0,2	0,3	0,3	0,3	0,2	0,2	0,2	0,2	0,2	0,2	0,2	0,2
0,2	0,2	0,2	0,2	0,3	0,3	0,3	0,3	0,3	0,4	0,3	0,3	0,3	0,3	0,3	0,2	0,2	0,2	0,2
0,2	0,2	0,2	0,2	0,3	0,3	0,3	0,3	0,3	0,4	0,3	0,3	0,3	0,3	0,3	0,2	0,2	0,2	0,2
0,2	0,2	0,2	0,2	0,3	0,3	0,3	0,3	0,3	0,4	0,3	0,3	0,3	0,3	0,3	0,2	0,2	0,2	0,2
0,2	0,2	0,2	0,2	0,3	0,3	0,3	0,3	0,3	0,4	0,3	0,3	0,3	0,3	0,3	0,2	0,2	0,2	0,2
0,2	0,2	0,2	0,2	0,3	0,3	0,3	0,3	0,3	0,4	0,3	0,3	0,3	0,3	0,3	0,2	0,2	0,2	0,2
0,2	0,2	0,2	0,2	0,3	0,3	0,3	0,3	0,3	0,4	0,3	0,3	0,3	0,3	0,3	0,2	0,2	0,2	0,2
0,2	0,2	0,2	0,2	0,3	0,3	0,3	0,3	0,3	0,4	0,3	0,3	0,3	0,3	0,3	0,2	0,2	0,2	0,2
0,2	0,2	0,2	0,2	0,3	0,3	0,3	0,3	0,3	0,4	0,3	0,3	0,3	0,3	0,3	0,2	0,2	0,2	0,2
0,2	0,2	0,2	0,2	0,3	0,3	0,3	0,3	0,3	0,4	0,3	0,3	0,3	0,3	0,3	0,2	0,2	0,2	0,2
0,2	0,2	0,2	0,2	0,3	0,3	0,3	0,3	0,3	0,4	0,3	0,3	0,3	0,3	0,3	0,2	0,2	0,2	0,2
0,2	0,2	0,2	0,2	0,2	0,2	0,2	0,2	0,3	0,3	0,3	0,2	0,2	0,2	0,2	0,2	0,2	0,2	0,2
0,2	0,2	0,2	0,2	0,2	0,2	0,2	0,2	0,3	0,3	0,3	0,2	0,2	0,2	0,2	0,2	0,2	0,2	0,2

TABLE II
PIEZOMETER DATA FOR THE FIVE-SPOT PATTERN INCLUDING ONE INJECTION WELL AND FOUR PRODUCTION WELLS

Pattern No	First	At Time	At Time	At Time	At Time	At Time	At Time	At Time	At Time	At Time	At Time	At Time
	0m	5 m	11 m	27 m	38:30 m	47 m	50 m	58:30 m	1 h 3 m	1 h 10 m	1 h 14 m	1 h 23 m
1	6,2	0	0	0	0	0	0	0	0	0	0	0
2	6,2	-4,8	-5	0,2	1,6	0,5	0,7	0,7	0,8	0,9	1	0
3	6,6	0	0	0	0	0	0	0	0	0	0	0
4	6	-3	6	7	4	3	3,4	3,4	3,5	3,5	3,4	1,5
5	6	12	15,5	12,8	10,5	9,9	8,6	8,5	8,9	8,5	8,3	4,5
6	6	-3,3	8,8	7,8	4,5	3,5	4	3,7	4,5	4	3,5	1,8
7	5,8	0	0	0	0	0	0	0	0	0	0	0
8	5,6	-4,5	-5	-2	-4,6	-0,6	0,4	0,5	1,3	1	1	-0,5
9	5	0	0	0	0	0	0	0	0	0	0	0
Up Stream	0	0	0	0	0	0	0	0	0	0	0	0
Down Stream	0	0	0	0	0	0	0	0	0	0	0	0

TABLE III
PIEZOMETER DATA FOR THE FIVE-SPOT PATTERN INCLUDING FOUR INJECTION WELLS AND ONE PRODUCTION WELL

Pattern No		A time	A time	A time	A time	A time	A time	A time	A time	A time	A time	A time	A time	A time	A time	A time	A time
	Fist time	1 min	4 min	9 min	13 min	17 min	21 min	25 min	29 min	35 min	40 min	45 min	50 min	56 min	1 hour	1h:10min	1h:19min
1	7	9,7	25	23	23	23	23	23	22,5	22,2	22,2	22	22	21,5	21,2	21,1	20,9
2	7,2	6,3	6,2	6,7	6,6	7	7	7	7,3	10,5	13,5	15,3	16	16,2	16,2	16,2	16,2
3	7,3	9,9	25	25	25	25	25	24,8	24,5	24,2	24	24	23,7	23,5	23	23	23
4	7,35	1,6	2,4	4	3,5	4,5	4,6	4,6	4,4	4	3,8	3,7	3,5	3,3	2,7	2,9	2,9
5	7,3	0	0	0	0	0	0	0	0	0	0	0	0	0	0	0	0
6	7,4	2,2	2,4	3,9	3,6	4,9	4,9	4,8	4,8	4,5	4,3	4,2	3,9	3,8	3,4	3,4	3,4
7	7,4	23	26	23	22,5	23	23	23	23	22,1	21,8	21,6	21,5	21	20,9	20,4	20,6
8	7,4	1,5	7,4	7,4	7,2	7,2	7,2	7,2	7,2	9,4	14,9	14,7	14,8	14,8	14,7	14,6	14,6
9	7,4	25	25	25	26	25	25	25,5	25,4	24,8	24,5	24,2	24	23,7	23,5	23,4	23,4
Up Stream	7,2	7,2	7,2	7,2	7,2	7,2	7,2	7,2	7,2	7,2	7,2	7,2	7,95	6,9	6,9	6,7	6,7
Down Stream	7	7	7	7	7	7	7	7	7	7	7	7	7	6,9	6,9	6,7	6,7

Fig. 12 (a) shows the five-spot pattern displacement of oil for four injection wells and one production well. The pink contour lines represent the equipotential pressure line in the reservoir and the blue line perpendicular to the equipotential line state is the streamline. The interpolation calculation is based on the piezometer data in Table III from the laboratory measurements (section II). Cross section (A-Á) (Fig. 12 (b)) is improved for the four injection wells to define the immiscible fluid relationship.

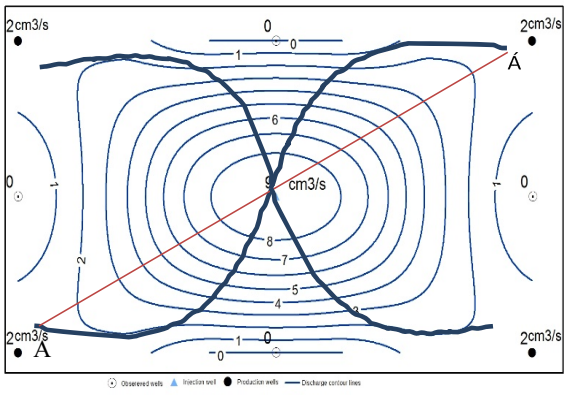

(a)

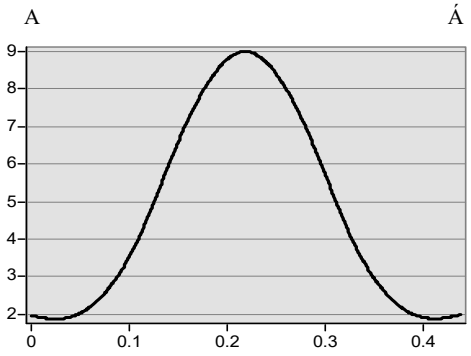

(b)

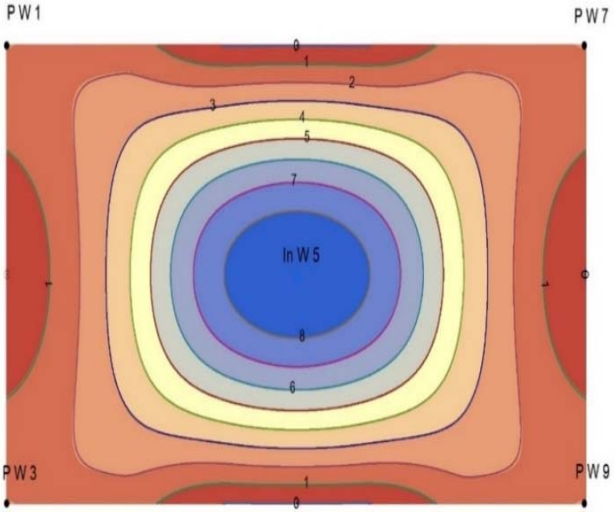

(c)

Fig. 11 (a) Schematic of water discharge contour lines of the five-spot quadrant side with a constant distance between the injection well and four production wells (b) Cross section of the equipotential line of dimensionless press (c) Water saturation contour lines with shaded areas for the five-spot quadrant side with a constant distance between the injection and production wells

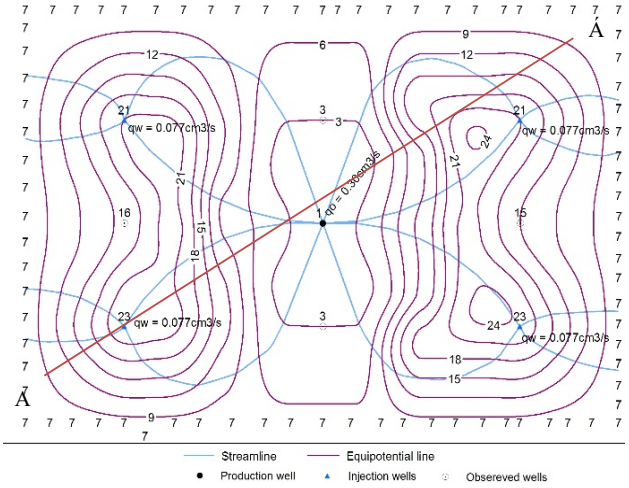

(a)

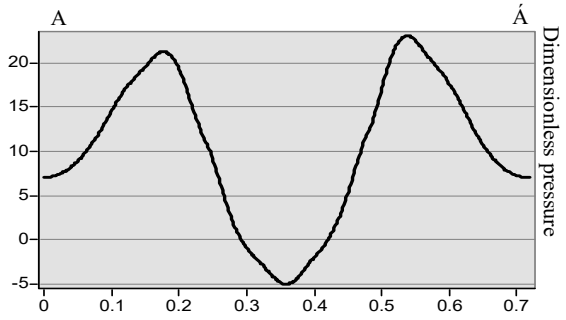

(b)

Fig. 12 (a) Scheme of equipotential line and streamlines of the five-spot quadrant side with constant distance between injection and production wells (b) Cross section of the equipotential line of dimensionless pressure.

X. Conclusion

A numerical simulation was used to obtain the solutions for pressure and water saturation equations to determine the pressure distribution and the water dispersion and distribution in two dimensions. A scaled laboratory model was used to measure the effect of the factors on water displacement during pumping. A five-spot pattern in a simulation model based on Darcy's law was used to create the injection and production wells system (Fig. 2). We predicted the water flooding mechanism by comparing the numerical simulation results with the laboratory measurements. The theory is typically used to treat fluid flow equations; however, we used Laplacian theory, which describes the dispersion and diffusion of fluid in two dimensions through the sand, under Darcy's law combined with Buckley-Leverett theory. The prediction of the saturation front was improved by the approximation method, in which the constant pressure points were connected (Figs. 11 (a)-(c) and 12 (a), (b)). When waterflooding is performed, the two main factors that must be controlled are water saturation and distribution in the reservoir, which requires the pressure to be

maintained during pumping. The immiscible displacement in two dimensions became complex. Analytically, it is sometimes difficult to solve this type of problem, but numerical simulations solved the most difficult immiscible reservoir equation that was presented in this paper. The finite difference method was used, which discretizes time and space and replaces the partial differential equations in the grid. The IADI method and IADE method were used because the equations for pressure and saturation were nonlinear. To develop an efficient recovery system, the pattern arrangement should be based on seismology information and geological investigation. Finally, a computer program was developed to speed up the calculation, and the results of pressure contour line were plotted (Fig. 11). However, for the saturation calculation, the program introduced errors into the partial differential equation. Thus, experimental piezometer data were used to plot interpolated equipotential lines, including the cross section, with approximation theory. Perpendicular to the equipotential lines, stream lines were drawn arbitrarily (Figs. 11 (a), 12 (b)), and the results showed good agreement with the laboratory measurements.

REFERENCES

[1] Buckley, S.E. and Leverett, M.C.: Mechanism of Fluid Displacement in Sands, Transactions AIME, Vol.146, pp.107-116 (1942).
[2] G. Paul Willhite, Waterflooding SPE Text Books Series pp 110-180 1986.
[3] By Staff, Offices of Mineral Resource: Potential Oil Recovery by Waterflooding Resevoirs Being Produced by Primary Methods,1970.
[4] Zhangxin Chen, Guaren Huan, Yuanle Ma Computational Methods for Multiphase Flows in Porous Media pp 465-480 2006.
[5] Chen Zgangxin, Reservoir Simulation Mathematical Techniques in Oil Recovery, University of Calgary, Calgary, Alberta, Canada, Copyright 2007 by the Society for Industrial and Applied Mathematics,. pp 25-50 1962.
[6] W. Donald. Peaceman Fundamentals of Numerical Reservoir Simulation pp 65-250 Copyright 1977.
[7] R. Allan Freeze/John A. Cherry, Groundwater pp.180-188. 1979.
[8] W. Kinzelbach, Groundwater Modelling an Introduction with Sample Programs in Basic, Vol. 25, pp.54-89. 1986.
[9] Elhassan Abdalla, Numerical Simulation of Pattern Miscible Displacement in a Heterogeneous with Varied Well Position pp 25-65 1990.
[10] R.V. Higgins and A.J. Leighton, Numerical Methods for Determining Streamlines and Isopressures for Use in Fluid-Flow Studies, Bureau of Mines Report 1972.